

## APPLIED SCIENCES AND ENGINEERING

# Comment on “Giant electromechanical coupling of relaxor ferroelectrics controlled by polar nanoregion vibrations”

P. M. Gehring<sup>1\*</sup>, Zhijun Xu<sup>1,2</sup>, C. Stock<sup>3</sup>, Guangyong Xu<sup>1</sup>, D. Parshall<sup>1</sup>, L. Harriger<sup>1</sup>, C. A. Gehring<sup>4</sup>, Xiaobing Li<sup>5</sup>, Haosu Luo<sup>5</sup>

Manley *et al.* (*Science Advances*, 16 September 2016, p. e1501814) report the splitting of a transverse acoustic phonon branch below  $T_C$  in the relaxor ferroelectric  $\text{Pb}[(\text{Mg}_{1/3}\text{Nb}_{2/3})_{1-x}\text{Ti}_x]\text{O}_3$  with  $x = 0.30$  using neutron scattering methods. Manley *et al.* argue that this splitting occurs because these phonons hybridize with local, harmonic lattice vibrations associated with polar nanoregions. We show that splitting is absent when the measurement is made using a different neutron wavelength, and we suggest an alternative interpretation.

Manley *et al.* (1) report neutron time-of-flight scattering measurements of the low-frequency lattice dynamics in the relaxor ferroelectric  $\text{Pb}[(\text{Mg}_{1/3}\text{Nb}_{2/3})_{1-x}\text{Ti}_x]\text{O}_3$  (PMN- $x$ PT) with Ti content  $x = 0.30$ . Above the Curie temperature  $T_C$  ( $\sim 405$  K), their data are consistent with a single transverse acoustic (TA) phonon branch measured at wave vectors  $\mathbf{Q} = (2 + H, H - 2, 0)$  for 0.0 rlu (reciprocal lattice units)  $< H < 0.4$  rlu. Below  $T_C$ , they observed a narrow dip in intensity located near the peak of the TA phonon line shape for  $H = 0.25$  rlu. This was interpreted as evidence that the TA phonon branch had split into two branches that exhibit anticrossing behavior.

We measured the neutron inelastic scattering from a 10-cm<sup>3</sup> single crystal of PMN- $x$ PT with nominally identical composition ( $x = 0.29$ ) below  $T_C$  for  $H = 0.25$  rlu, i.e., at a constant wave vector  $\mathbf{Q} = (2.25, -1.75, 0)$ . These data were obtained using the National Institute of Standards and Technology (NIST) BT7 triple-axis spectrometer, which selects the incident and final neutron energies via Bragg diffraction rather than time of flight, but instead of collecting data with a fixed incident neutron energy of  $E_i = 25$  meV as performed in (1), we used a commonly used fixed final neutron energy  $E_f = 14.7$  meV. Our data, as shown in Fig. 1 (top), show no evidence of this splitting. A least-squares fit to a single damped harmonic oscillator describes the TA phonon extremely well.

This result raises the question of why the TA phonon splitting is seen in the configuration used by Manley *et al.* (1) ( $E_i = 25$  meV) but not in the one used by us ( $E_f = 14.7$  meV). We can explain why quantitatively via a double scattering process involving a phonon and a Bragg peak. Spurious features generated in this manner were termed “ghostons” by Rønnow *et al.* (2) and used successfully to explain unexpected features observed in the neutron inelastic scattering from  $\text{CuGeO}_3$ . In Fig. 1 (bottom), we have replotted data published by Manley *et al.* (1) using the same energy scale to facilitate comparison between our datasets. Note that our data are plotted on a linear intensity scale, whereas those of Manley *et al.* (1) are plotted on a log scale. We calculated ghoston energies for the case when  $E_i =$

25 meV using only the measured cubic lattice constant of 4.02 Å. The energies of three ghostons (red arrow) coincide precisely with the anomalous intensity dip seen in the data for  $H = 0.25$  rlu (purple open circles), and each follows the dip to higher energy as  $H$  decreases. These are generated via scattering from phonons located at  $\mathbf{Q} - \boldsymbol{\tau} = (0.25, -1.75, -2)$ ,  $(0.25, -1.75, 2)$ , and  $(-1.75, -1.75, 0)$ , respectively, followed by Bragg scattering from the reciprocal lattice vectors  $\boldsymbol{\tau} = (2, 0, 2)$ ,  $(2, 0, -2)$ , and  $(4, 0, 0)$ . Only the first two ghostons will contribute substantially because the last involves a longitudinal acoustic phonon at much higher energy. Ghostons can add or subtract intensity from a given location in reciprocal space; the magnitude and sign of the excess intensity depends on the sample and scattering geometries (3). In this case, the “Bragg-last” ghostons reduce the intensity at this energy, thereby producing a dip in the TA phonon line shape. It is important to note that this dip is less apparent below and above  $H = 0.25$  rlu. Our model captures this behavior because these ghostons and the TA phonon disperse in opposite directions. That is, the TA phonon splitting seems weaker (or absent) at lower/higher  $H$  because the ghostons overlap less with the TA phonon.

The following three questions remain: (i) Why does this feature vanish above  $T_C$ ? (ii) Why is it observed in the  $(1\bar{1}0)$  Brillouin zone? (iii) Why is it affected by an external electric field? The answers are (i) primary extinction (4), (ii) ghostons exist in all zones (2), and (iii) electric fields strongly affect PMN- $x$ PT Bragg intensities (5). In the cubic perovskite structure, Bragg reflections having all even Miller indices ( $hkl$ ) have the largest structure factor. Therefore, they (and all related ghostons) suffer the greatest extinction on heating above  $T_C$  (4). This effect is large: The (200) Bragg intensity in our crystal decreases by a factor of six between 300 and 500 K. In the  $(1\bar{1}0)$  zone, several ghostons have energies close to those in the  $(2\bar{2}0)$  zone for  $E_i = 25$  meV, including the Bragg-first ghostons generated by  $\boldsymbol{\tau} = (1, 3, \pm 1)$ . Moreover, as shown in Fig. 2, we observed no TA splitting at  $\mathbf{Q} = (1.25, 0.75, 0)$ , when  $E_f = 13.7$  meV (another common configuration). Thus, the splitting in this zone is also wavelength dependent. Last, applied electric fields are known to affect Bragg intensities (5); for this reason, they necessarily affect any associated ghoston intensities.

Elastic-inelastic double scattering processes are generally extremely weak, but Rønnow *et al.* (2) note that even 1-cm<sup>3</sup> crystals can produce ghostons. As the PMN- $x$ PT crystal used by Manley *et al.* (1) has a volume of order of 20 cm<sup>3</sup>, these effects should be expected. Scattering studies of large single crystals of relaxors are particularly problematic: The unusually broad phonon energy widths greatly enhance the chances

<sup>1</sup>NIST Center for Neutron Research, National Institute of Standards and Technology, Gaithersburg, MD 20899-6100, USA. <sup>2</sup>Department of Materials Science and Engineering, University of Maryland, College Park, MD 20742, USA. <sup>3</sup>School of Astronomy and Physics, University of Edinburgh, Edinburgh EH9 3JZ, UK. <sup>4</sup>Computer Science and Artificial Intelligence Laboratory, Massachusetts Institute of Technology, Cambridge, MA 02139, USA. <sup>5</sup>Shanghai Institute of Ceramics, Chinese Academy of Sciences, Shanghai 201800, China.

\*Corresponding author. Email: peter.gehring@nist.gov

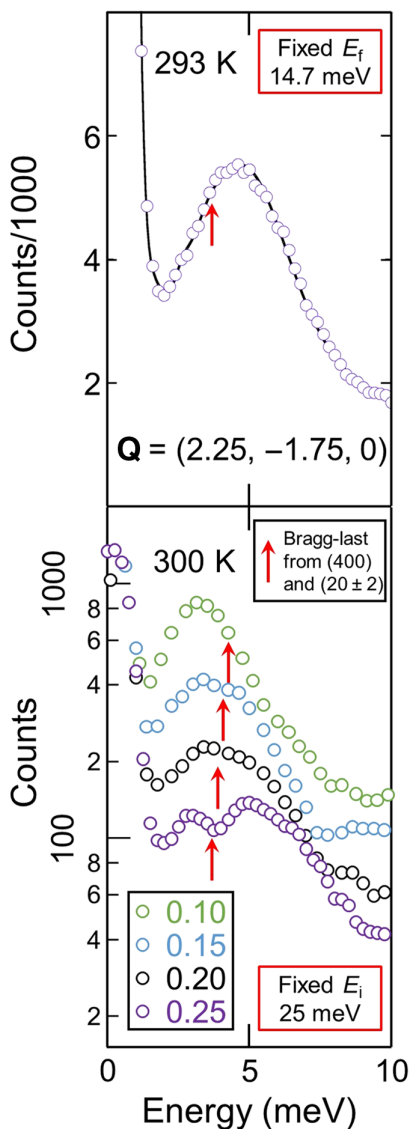


**Fig. 1. TA mode in (220) Brillouin zone.** (Top) Energy scan at  $\mathbf{Q} = (2.25, -1.75, 0)$  showing an unsplit TA phonon line shape in PMN-xPT with  $x = 0.29$ . The solid line is a fit to a single damped harmonic oscillator. Data were measured with  $E_f = 14.7$  meV. Errors bars represent  $\pm\sqrt{N}$ , where  $N$  is the total number of counts. (Bottom) Energy scans from Manley *et al.* (1) for  $\mathbf{Q} = (2 + H, H - 2, 0)$  using  $E_i = 25$  meV. The ghoston energy is indicated by a red arrow for each value of  $H$ .

of observing ghostons because the strict constraint imposed by energy conservation is much easier to satisfy (6).

We have shown that the purported TA phonon splitting depends on the choice of neutron energy. We can account for this anomaly quantitatively using an inelastic double-scattering model. Thus, we believe that the TA phonon splitting reported by Manley *et al.* (1) is spurious.

## MATERIALS AND METHODS

We studied an 80-g single crystal of PMN-xPT with nominal Ti content  $x = 0.29$ . The crystal was cut with {100} faces and dimensions of 17.8 mm by 23 mm by 24.3 mm. The crystal was loaded into an alu-

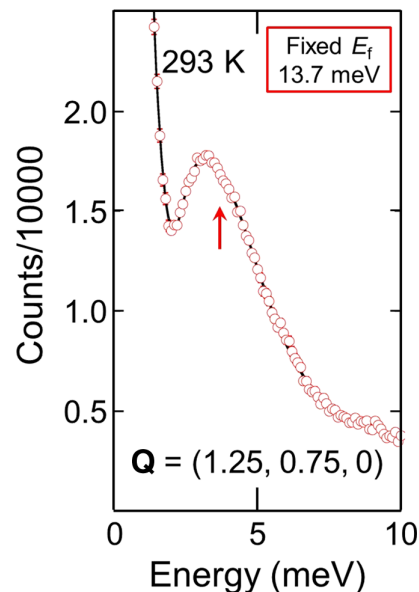


**Fig. 2. TA mode in (110) Brillouin zone.** Energy scan at  $\mathbf{Q} = (1.25, 0.75, 0)$  in PMN-xPT with  $x = 0.29$ . The solid line is a fit to a single damped harmonic oscillator line shape. These data were measured on the NIST BT4 triple-axis spectrometer with  $E_f = 13.7$  meV. Errors bars represent  $\pm\sqrt{N}$ , where  $N$  is the total number of counts.

minum sample can in the (HK0) scattering plane with [100] parallel to the 17.8-mm dimension and mounted inside a closed-cycle  $^4\text{He}$  refrigerator. Data on the NIST BT7 triple-axis spectrometer were measured at constant wave vector  $\mathbf{Q}$  by varying the incident neutron energy while holding the final neutron energy  $E_f$  fixed at 14.7 meV. Horizontal beam collimations of  $120' - 80' - 80' - 120'$  were used. A neutron velocity selector located before the monochromator eliminated higher-order neutrons from the incident beam; a highly oriented pyrolytic graphite filter was placed in the scattered beam. Similar measurements were carried out on the NIST BT4 triple-axis spectrometer using a fixed final neutron energy of 13.7 meV and no velocity selector. We calibrated the BT7 and BT4 wavelengths and scattering angles using an alumina standard and aligned the analyzers using vanadium, which is an incoherent scatterer.

## REFERENCES AND NOTES

1. M. E. Manley, D. L. Abernathy, R. Sahul, D. E. Parshall, J. W. Lynn, A. D. Christianson, P. J. Stohara, E. D. Specht, J. D. Budai, Giant electromechanical coupling of relaxor ferroelectrics controlled by polar nanoregion vibrations. *Sci. Adv.* **2**, e1501814 (2016).
2. H. M. Rønnow, L.-P. Regnault, J. E. Lorenzo, Chasing ghosts in reciprocal space—A novel inelastic neutron multiple scattering process. *Physica B* **350**, 11–16 (2004).
3. R. M. Moon, C. G. Shull, The effects of simultaneous reflections on single-crystal neutron diffraction intensities. *Acta Crystallogr.* **17**, 805–812 (1964).
4. G. E. Bacon, R. D. Lowde, Secondary extinction and neutron crystallography. *Acta Crystallogr.* **1**, 303–314 (1948).
5. S. B. Vakhruшев, B. E. Kvyatkovsky, A. A. Naberezhnov, N. M. Okuneva, B. P. Toperverg, Glassy phenomena in disordered perovskite-like crystals. *Ferroelectrics* **90**, 173–176 (1989).
6. P. M. Gehring, D. Parshall, L. Harriger, C. Stock, G. Xu, X. Li, H. Luo, Correspondence: Phantom phonon localization in relaxors. *Nat. Commun.* **8**, 1935 (2017).

**Acknowledgments:** P.M.G. acknowledges useful communications with Michael E. Manley.  
**Funding:** The authors acknowledge that they received no funding in support of this work.

**Author contributions:** P.M.G. conceived experiments. P.M.G., C.S., and G.X. performed neutron scattering measurements on BT4. P.M.G., Z.X., and D.P. performed those on BT7. P.M.G. analyzed all scattering data. P.M.G., L.H., and C.A.G. performed ghoston model calculations. X.L. and H.L. grew the single crystals. P.M.G. wrote the manuscript with input from all authors. **Competing interests:** The authors declare that they have no competing interests. **Data and materials availability:** All data needed to evaluate the conclusions in the paper are present in the paper. Additional data related to this Technical Comment may be requested from the corresponding author.

Submitted 1 May 2018  
Accepted 14 February 2019  
Published 22 March 2019  
10.1126/sciadv.aar5066

**Citation:** P. M. Gehring, Z. Xu, C. Stock, G. Xu, D. Parshall, L. Harriger, C. A. Gehring, X. Li, H. Luo, Comment on "Giant electromechanical coupling of relaxor ferroelectrics controlled by polar nanoregion vibrations". *Sci. Adv.* **5**, eaar5066 (2019).

## Comment on “Giant electromechanical coupling of relaxor ferroelectrics controlled by polar nanoregion vibrations”

P. M. Gehring, Zhijun Xu, C. Stock, Guangyong Xu, D. Parshall, L. Harriger, C. A. Gehring, Xiaobing Li, and Haosu Luo

*Sci. Adv.* **5** (3), eaar5066. DOI: 10.1126/sciadv.aar5066

### View the article online

<https://www.science.org/doi/10.1126/sciadv.aar5066>

### Permissions

<https://www.science.org/help/reprints-and-permissions>

Use of this article is subject to the [Terms of service](#)

---

*Science Advances* (ISSN 2375-2548) is published by the American Association for the Advancement of Science, 1200 New York Avenue NW, Washington, DC 20005. The title *Science Advances* is a registered trademark of AAAS.

Copyright © 2019 The Authors, some rights reserved; exclusive licensee American Association for the Advancement of Science. No claim to original U.S. Government Works. Distributed under a Creative Commons Attribution NonCommercial License 4.0 (CC BY-NC).